beverages

MDPI

Article

Coarse-Grained Molecular Dynamics Simulations for Predicting Rheological Behavior of Casein Micelle Dispersions

Raghvendra Pratap Singh [1], Sophie Barbe [2], Paulo Peixoto [1], Manon Hiolle [3,*], Frédéric Affouard [1] and Guillaume Delaplace [1]

[1] University of Lille, CNRS, INRAE, Centrale Lille, UMR 8207, UMET, Unité Matériaux et Transformations, 59000 Lille, France; pratapiids@gmail.com (R.P.S.); paulo.peres-de-sa-peixoto-junior@inrae.fr (P.P.); frederic.affouard@univ-lille.fr (F.A.); guillaume.delaplace@inrae.fr (G.D.)
[2] Toulouse Biotechnology Institute (TBI), Université de Toulouse, CNRS, INRAE, INSA, 31077 Toulouse, France; sophie.barbe@insa-toulouse.fr
[3] Ingredia Dairy Experts, 62000 Arras, France
* Correspondence: m.hiolle@ingredia.com

Abstract

Handling dispersion of casein powders in water is widely encountered in the milk industry. However, in silico prediction of the apparent viscosity of these colloidal dispersions is not an easy task, especially when these micellar casein suspensions are highly concentrated, as in hyper-protein milk beverages, which are experiencing exponential market growth. In this work, Coarse-Grained (CG) models using Lennard-Jones potentials to model interactions were built for simulating rheological properties of colloidal micellar casein dispersions (native and demineralized). In a first approach, a polydisperse explicit CG model was developed. For this polydisperse CG model, the representation chain was composed of four large smooth spheres of different sizes mimicking the real distribution of casein colloids. The CG simulation results were validated by comparison with experimental rheological data for native colloidal casein dispersions. Both in-house experimental results and available data found in the literature were used for this purpose, covering a wide range of casein concentrations ([10 g/L–200 g/L], [8–20%] corresponding to casein concentration, colloid volume fraction and solid/liquid volume fraction, respectively). In a second approach, a simplified model using a monodisperse CG model was developed. This simplified model only included one type of soft sphere and was found to preserve the accuracy of the rheological prediction. Finally, a monodisperse CG model was set up to predict the behavior of demineralized micellar casein dispersions, for which a decrease in the average size of the micelle size distribution is observed when demineralization occurs. For all models, the comparison between the predicted and experimental rheological behavior is fully satisfactory, proving that the CG models proposed for casein-based micellar dispersions are physically well founded and that the proposed simplified representation chain, based on micelle size observation, makes sense.

Keywords: casein; coarse-grained model; rheology; colloids

Check for updates

Academic Editors: Edgar Chambers IV and Guadalupe Garcia-Llatas

Received: 3 October 2025
Revised: 1 December 2025
Accepted: 13 January 2026
Published: 6 February 2026

Copyright: © 2026 by the authors. Licensee MDPI, Basel, Switzerland. This article is an open access article distributed under the terms and conditions of the Creative Commons Attribution (CC BY) license.

1. Introduction

The worldwide dairy industry produces millions of tons of cow's milk powders annually and turns them into powders such as skimmed milk powder, whole milk powder, lactoserum powder, and whey protein isolate powder, as Lagrange et al. underlined [1]. The manufacture of powders from liquid milk was initiated more than a century ago

as a solution for extending milk products' shelf life during storage and for facilitating their transport thanks to the elimination of water. Milk powder manufacture is mainly carried out through spray drying of milk protein concentrates after previous pasteurization/evaporation/filtration steps on milk; however other drying routes to obtain powders such as drum and freeze drying are also encountered in the food and dairy sectors [2]. This "water-free preservation" technique means that the redispersion of milk powders in water to obtain dairy derivatives has become a frequent and very common step in the food industry. This rehydration step is sometimes accompanied by the addition of various ingredients (salts, lactose, fat, etc.) through a series of thermo-mechanical unit operations, in order to texturize and sanitize the targeted foodstuffs with the desired level of quality.

Although the redispersion step of milk powder in aqueous solvents is widespread, little has been achieved in understanding and in modeling it. Until now, little is known about how these protein and mineral compounds contained in the powders interact with each other and how these interactions are supposed to impact some future functional properties of milk dispersions after rehydration. This work seeks to provide insights into this area. In particular, simulations based on Coarse-Grained (CG) protein models are proposed for describing the dispersion in water of various micellar casein powders and for predicting the rheological properties of dispersed solutions at the end of the rehydration step. This study was carried out at various solid/liquid ratios (1–200 g/L) and for different kinds of protein powders obtained by spray drying, namely, different micellar casein concentrates (called native or demineralized) at the end of the rehydration step. The goal is twofold. We would like to highlight that such a modeling approach can be performed for complex soft and edible materials like milk and can provide useful information for predicting end-use properties of casein dispersions expected by users. Note that in this work, casein dispersions were made by powder rehydration, which were all spray-dried from a concentrate. The term "native" therefore refers here to a concentrate that has not been demineralized.

Casein powders have been selected in our work as they are widely recognized as a pivotal source of dietary protein and minerals [3–8] and are frequently used in the manufacture of conventional dairy products such as cheese [9], yoghurt [10,11], and food supplements [12]. For many applications, it is asserted that milk powders should be completely dispersed in an aqueous medium to fully exhibit their functional properties. Consequently, for ingredient users, the dispersibility of a protein powder is a critical attribute [13]. Moreover, the mastering of rehydration for micellar casein powders is known to be harder and more challenging than for whey protein powders, which are more easily solubilized in the aqueous phase [14,15], and until today, persistent efforts have been made by dairy powder manufacturers to find a way to improve the rehydration ability of casein-based powders and elaborate more instant powders as recently reported by McSweeney et al. [16].

Casein proteins are the main source of proteins in cow's milk (approximately 80% of total protein content). Recently, the incorporation of more milk proteins into nutrition and health products has increased significantly [17], namely, in Hyper-Protein beverages (HPs) [18–21]. In this context, casein micellar powder represents one of the most interesting sources of proteins for ready-to-drink HP beverages due to its high availability and heat resistance. These HP drinks are commonly used to maintain health and accelerate recovery in ill patients suffering from cancer [22] or to increase muscle mass in athletes, body builders [23,24], or the elderly population affected by sarcopenia [25]. For these micellar casein-based HP beverages, low viscosity is a key functional property desired by consumers for their daily liquid protein intakes. The casein micelle (CM) concentration plays an important role in the viscosity of dispersions. Indeed, it is known that CMs

have an important apparent voluminosity and consequently promote higher viscosity for dispersions. However, an in-depth understanding on how the concentration and the structure of micellar casein regulate the rheological behavior of dispersions is still required. In addition, some strategies have been proposed to produce structural changes in casein, which result in dense dispersions with altered apparent viscosity, such as calcium demineralization [26,27]. Nevertheless, some interesting properties of the demineralized CMs have been observed [21,28–30]. For chemical engineers, faced with the increasing demands of formulating HP beverages, it is also vital to improve knowledge on predicting the rheological properties of CM dispersions after each unit operation of the processing line, including the preliminary reconstitution step before heating. Indeed, apparent viscosity is a key parameter that limits the transport phenomena (flow, heat, and mass), and knowledge of this property is necessary to properly design process equipment and optimize process operations.

Milk, in its native state, contains four type of casein proteins: caseins-αs1 (αs1-CN), αs2 -casein (αs2-CN), β-casein (β-CN), and κ-casein (κ-CN), which have molecular weights between 19 and 25 kDa and an average isoelectric point between 4.1 and 5.3 [31]. These proteins are found in the proportion of 3:1:3:1. The milk is also composed of mineral, with approximately 8% by mass consisting of phosphate and calcium ions. In native milk, the casein molecules are associated together to form casein micelles. Casein micelles form a high-order organized protein assembly where individual caseins and minerals contained in colloidal calcium phosphate clusters (CCPs) interact [32–35]. Casein micelles are stabilized and linked together through interactions between phosphoryl groups from the post-translation (phosphorylation) modification of serine residues and internal CCPs [7,32,34]. Native micelles size ranges from ~50 nm (mini-micelle) to up to ~500 nm (a supra-molecular micellar assembly) [33,36–38]. The predominant casein micelle size falls between ~50 and 300 nm with an average micellar size of ~150 nm [20,39,40]. Native micelles can therefore be considered nanoparticles.

The micellar assembly of caseins at the molecular scale has been studied for almost 50 years. Despite these extensive studies, the nature of this micellar structure remains unclear and multiple conflicting models have been proposed for the casein micellar structure. The most widely accepted model is now considered as a roughly spherical "core–shell" [7,30,32,35,38,39,41,42], in which α-s1, α-s2, and β-casein together with CCPs form the core of the micelle and κ-casein forms an outer corona or polyelectrolyte brush, producing s short-range repulsion between micelles and participating in its stabilization by electrostatic and steric repulsion [39,43,44]. Furthermore, despite the variety of the proposed models, most studies and models agree on the cementing and bridging role of CCPs, which are bound to caseins through the negative charges of the carboxylate groups of Glu and Asp and through the phosphate group of SerP. These studies have illustrated to some extent that casein micelles behave as interactive particles. CCPs can be extracted from a micellar casein concentrate by applying different thermo-mechanical or physico-chemical conditions altering the structure and techno-functionalities of casein micelles both in the concentrates and in the powder obtained after spray drying [45–47]. Demineralized casein micelle powders obtained through acidification and filtration processes are such examples and are reported to exhibit different rehydration and viscosity properties after redispersion in water. Moreover, Nogueira et al. [30,46–48], who compared the sizes of native and demineralized micelles, reported that upon demineralization, casein micelles can either swell or shrink depending on the degree of demineralization. From SAXS experiments [30], diameters ranging from 204.5 nm to 230 nm for demineralized caseins were found, whereas the diameter of native caseins is close to 208 nm, which is consistent with the literature [49].

Flow properties of colloidal suspensions have been widely addressed in the rheology community. However, most of the fundamental studies on the rheological behavior of these suspensions have used "hard spheres" (considered as rigid and non-interactive particles) with a monomodal diameter as colloids. Most of the investigations deal with colloids dispersed at low volume fractions below 0.5 (volume occupied by the number of colloids in the unit cell divided by the volume of a unit cell), which are far away from random close packing of monodisperse (0.64) or 40% polydisperse hard-sphere fluid (0.78). These studies are far from being representative of situations encountered in the HP casein-based beverage sector (high-volume fractions, nanocolloids, interactive, non-spherical, etc.). Moreover, for these specific dispersions, a micelle size distribution (rarely known a priori) exists, and casein micelles are widely admitted to be deformable particles. This is definitely proven, as the effective volume fraction of casein dispersion (obtained by multiplying the casein concentration in g/L by a factor that accounts for the voluminosity of the casein in the suspending medium) for an HP beverage can be superior to 0.64, which is the limit for rigid spheres. This effective volume fraction value, corresponding to the maximum volume fraction to pack randomly hard perfect same-size spheres, is reached when the casein concentration exceeds 145 g/L (estimated using a micelle voluminosity of 4.4 mL/g by Bouchoux et al. [50]).

These works were motivated by the experimental work of Bouchoux et al. [50] and Dahbi et al. [51], who measured the rheological behavior of native casein micelle dispersions at different casein concentrations in order to obtain information on the micelle interactions below and above random close packing. Specifically, the work of Bouchoux et al. [50] was carried out for casein concentrations expressed in g/L as casein powder weight per volume, ranging from 10 to 168 g/L, while the work of Dahbi et al. [51] was performed with native casein micelle dispersions expressed in casein weight percent, ranging from 1.14% *w*/*w* to 19.1% *w*/*w*.

Analysis of their results showed that micellar casein dispersions can adopt different rheological behaviors, depending on the values of the effective volume fraction of the casein. Precisely, for casein concentrations below 170 g/L, it has been shown that the dispersions could be regarded as purely viscous liquids (without or with few elastic properties), displaying Newtonian to shear thinning behavior driven by increasing casein concentration. For casein concentrations below 170 g/L and at low shear rates, the viscosity behavior can be modeled by considering the hard-sphere type of interaction, whereas a deviation appears when the volume fraction approaches random close packing and at high shear rates, presumably caused by micelle deformations in the flow. For these cases, the flow properties indicate that the micelles are well separated from each other and interact only through excluded volume effects. A drastic increase in viscosity and rise in elastic properties are observed at a higher casein concentration above random close packing. A liquid–solid transition is progressively observed. As in the polymeric matrix, it is obvious that further research is needed to clarify how fillers affect the elastic properties, but it is not the target of this study.

The molecular simulation field has considerably progressed since its advent. Today, a wide range of computational techniques, particle diffusion, and self-assembly theoretically based rules are available to describe how colloidal particles, such as protein and other ingredients (mineral, fat, carbohydrates) dispersed in a solvent interact [52]. It includes Dissipative Particle Dynamics (DPD) [53,54], the Lattice Boltzmann (LB) method [55], Brownian dynamics (BD) [56,57], Stokesian dynamics (SD) [58], Stochastic rotation dynamics (SRD) [59], and fast lubrication dynamics (FLD) [60]. Therefore, it is conceivable, based on knowledge of milk derivative composition, to study how these user-imposed colloidal strengths lead to intermediate aggregates or transient particle clusters, and then, after

inducing additional interparticle hydrodynamic forces, result in a final structure and rheology of colloidal systems. Unfortunately, quantitative information on the precise form of the model that should be defined for casein dispersions is generally unavailable.

The aim of our study is to partially fill this gap. Firstly, an implicit CG solvent model (called the polydisperse CG model) has been developed to computationally predict the colloidal assembly at equilibrium when concentrated micellar powders are dispersed under isothermal temperature. Then, this first CG model has been assessed by testing its ability to predict the rheology of dilute to dense casein micelle suspensions. In particular, validation will aim to check whether the simulated change in rheological properties due to critical packing when the casein concentration increases could be satisfactorily predicted. For that, experimental rheological data, obtained by our group [30,46,47] and in the literature [50], will be used. Secondly, we will show that the polydisperse CG model could be simplified by a monodisperse CG model, easier to set in place, as the distribution of particle size for casein micelles is rarely known a priori. The ability of this monodisperse CG model to predict the rheological properties of demineralized casein dispersions, for which a decrease in the average casein dimension is observed, will be discussed.

2. Materials and Methods

Coarse-Grained numerical models

For all models, the interactions between colloidal particles were modeled by the purely repulsive Lennard-Jones (LJ) potential, also known as the Weeks–Chandler–Andersen (WCA) potential:

$$\begin{cases} U_{WCA}(r) = 4\varepsilon\left[\left(\frac{\sigma}{r}\right)^{12} - \left(\frac{\sigma}{r}\right)^{6} + \frac{1}{4}\right],\ r \leq rc = 2^{\frac{1}{6}}.\ \sigma \\ U_{WCA}(r) = 0,\ \ r > rc \end{cases}$$

where ε is the interaction well depth (energy minimum), σ is the distance at which the potential becomes zero, r is the distance between two interacting particles, and rc is the cutoff distance for interactions. The Lennard-Jones potential is a well-studied common pair potential, which contains a repulsive wall when particles approach each other and a long attractive tail. The WCA potential is essentially a shifted LJ potential without an attractive tail. The WCA potential is commonly used to simulate particle interactions, which have softer repulsion than rigid spheres but no attractions.

In a first approach, it was assumed that the interactions occurring between the dispersed colloidal–proteinaceous system would be satisfactorily described if the micellar casein particle size distribution were approximated as a set of spherical soft colloidal particles of different diameters immerged in an implicit solvent model (Figure 1).

"Implicit solvent" refers to models in which the solvent is not represented by individual molecules. Instead, its influence is included through a mathematical model that treats the solvent as a continuous medium. This approach contrasts with explicit solvent simulations, where solvent molecules are added and their interactions are computed directly. Implicit solvent models approximate solvent effects such as electrostatic screening, hydrophobic forces, and the overall dielectric environment. Because the solvent is not simulated atom by atom, implicit solvent MD runs much faster. However, it is less accurate in situations where detailed solvent structure or specific solvent-mediated interactions are important.

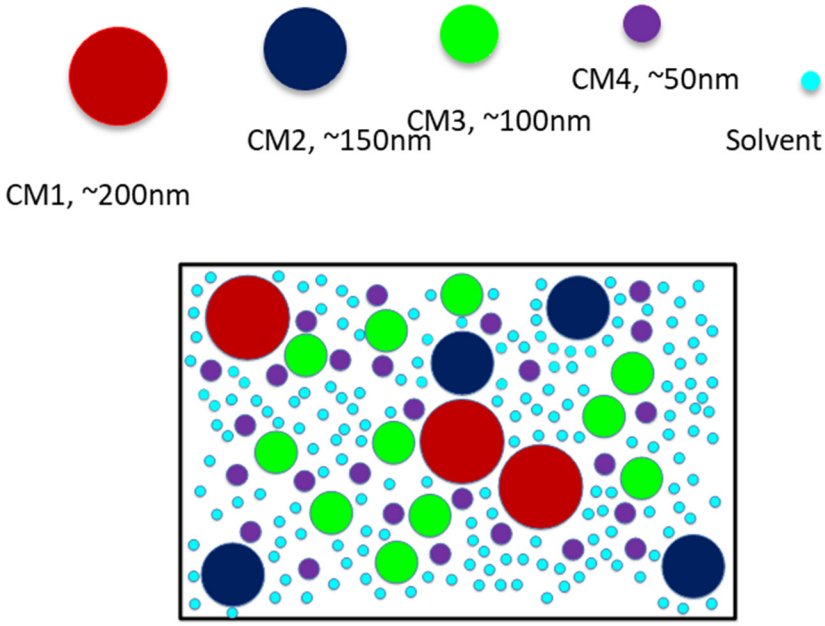


Figure 1. Simplified representation chain (polydisperse CG representations) for mimicking suspensions of native phosphocasein micelles at various colloidal concentrations. Solvent particles are treated implicitly.

The colloidal–proteinaceous particles were represented by large soft spheres of 4 different sizes: 50, 100, 150, and 200 nm in diameter (CMi with i from 1 to 4), while solvent particles were modeled implicitly (Figure 1). The σ parameter of the WCA potential is adjusted to match the soft spheres' diameter (see Table 1). The number of large soft spheres (CMi with i from 1 to 4) is approximately 35, 509, 920, and 536, respectively. In contrast to Devarajan et al. [61], solvent molecules have been treated implicitly for simplicity and to accelerate computations. Different volume fractions of colloidal particles were considered, ranging from 8% v/v to 20% v/v.

Table 1. Pair interaction potential parameters for the polydisperse CG models used in the simulations.

Interaction Between CMi and CMj Particles	ε (kcal/mol)	σ (nm)
1-1	3.10	200
1-2	2.71	175
1-3	2.32	150
1-4	1.94	125
2-2	2.32	150
2-3	1.94	125
2-4	1.55	100
3-3	1.55	100
3-4	1.16	75
4-4	0.77	50

In a second approach, the representation chain chosen to mimic the casein dispersions was a monodisperse CG model, which explicitly accounted for a single micellar casein particle size (CMi with i = 1). As in the previous model, the background solvent particles were modeled implicitly and the colloidal particles were treated as large smooth spheres.

MD simulations were performed for different average colloidal particle sizes ranging from 196 to 215 nm, adjusting accordingly the σ parameter of the WCA potential. For the different simulations, the viscosity was calculated and compared to the experimental value in order to estimate the best particle size. Using the same methodology, other simulations were carried out for casein dispersions at 5%, 10%, 25% demineralization, using different particle sizes.

The CG models described in the above sections were used to perform molecular dynamics (MD) simulations using the LAMMPS MD package [62,63]. A 3D cubic simulation box of edge length L = 25 μm was used for all the MD simulations carried out. The volume fraction of colloidal suspensions in the central simulation box was defined as $\varphi = (N_(c,i)/V).(4/3).\pi(R_(c,i))^3$, where N_(c,i) accounts for the number of type i colloidal particle in the simulation box, R_(c,i) is the radius of type i colloidal particles, and V is the volume of the simulation box. The number of colloidal particles varied from Nc = 2000 to 200,000 for volume fractions ranging from 8% to 20%, respectively. Two types of MD simulation were performed. First, a preliminary MD run was carried out in the NVT statistical ensemble to thermalize the system at the target temperature (T = 25 °C). Then, the subsequent production MD runs (from which the viscosity is calculated) were performed in the NVE ensemble. The systems were equilibrated for a period of 10^{-5} s using a time step of 1 ps.

Steady shear simulations were carried out using the non-equilibrium Molecular Dynamic simulations (NEMD) technique [64]. This was achieved by applying the sliding-brick periodic boundary conditions on the simulation box and using the SLLOD equation of motion [61,64–66]. The NEMD simulations were performed at different shear rates from 10 to 500 s^{-1} and at temperatures of 25 °C and 50 °C, aiming to identify both the rheological behavior of the casein dispersion with respect to casein concentration and the effect of temperature on the viscosity values of casein dispersions.

Experimental data

Experimental data were extracted from Nogueira's PhD thesis [47], and complementary details can also be found in subsequent publications [30,46,48]. For the sake of clarity, the main material and methodological elements are summarized below.

Casein-based powders (called "Native" or "Demineralized") were provided by Ingredia S.A (Arras, France). The percentage of calcium demineralization of each powder was measured as indicated in Nogueira et al. [30,47]. The powders were rehydrated to the desired casein weight percent ranging from 8% *w*/*v* to 20% *w*/*v* and homogenized as indicated in Nogueira et al. [30]. Shortly, the casein-rich powders were rehydrated with deionized water to the desired casein concentration under stirring at 500 rpm at 50 °C/1 h. Three drops of antifoam silicone solution were added to each powder dispersion at the beginning of rehydration to prevent foam formation. The pH was adjusted to 7.0 with NaOH 1 M. After pH adjustment, the samples were homogenized at 10,000 rpm for 5 min using a rotor-stator homogenizer, Polytron PT 10-35a (Kinematica, Malters, Switzerland). This homogenization process was applied with the aim of breaking up any remaining aggregates. The apparent viscosity was measured using a Couette geometry, using an AR 2000ex Rheometer (TA Instruments, Guyancourt, France) equipped with a coaxial cylinder (internal radius = 14 mm, external radius = 15 mm, cylinder height = 42 mm). Experiments were conducted at 50 °C and at 25 °C, varying the shear rate from 10 to 500 s^{-1}.

To further evaluate the robustness of CG models developed in this study, additional simulations were performed in order to predict the rheological behaviors of casein dispersions previously handled by Bouchoux et al. [50]. In this work, casein concentration is expressed in g/L as casein powder weight per volume and varies from 10 to 168 g/L. However, even if all experiments were obtained with dispersions made by rehydrating

Phosphocaseinate powder (PPCN) powder at various casein powder weights per volume, significant differences exist between the experimental protocols of Nogueira et al. and Bouchoux et al. [47,50]:

- The technological route to obtaining the PPCN powder from the concentrate (indicated in the original publication) was not fully the same. Moreover, the initial dairy ingredients were not delivered by the same manufacturer (Protarmor instead of Ingredia).
- The rehydration conditions were also significantly different: the solvent for redispersing powder is made from ultrafiltration of skimmed milk (UF permeate) instead of deionized water, and the duration of the rehydration protocol was also different (15 h at 35 °C and 50 °C, respectively, instead of 1 h at 50 °C).
- The rheological devices to measure the viscous properties were also different.

3. Results and Discussion

3.1. Comparison Between Simulated and Experimental Rheological Data for PPCN Dispersions Using the Polydisperse CG Model

The apparent viscosity evolution with shear rate of "native" PPCN dispersions obtained experimentally and simulated by the CG polydisperse model is shown in Figure 2. The different colors of symbols correspond to two solvent temperature conditions (25°C or 50 °C) and different casein weights per volume, expressed as a percentage (8% *w*/*v*, 14% *w*/*v* and 20% *w*/*v*). These data were published in [30,46,48].

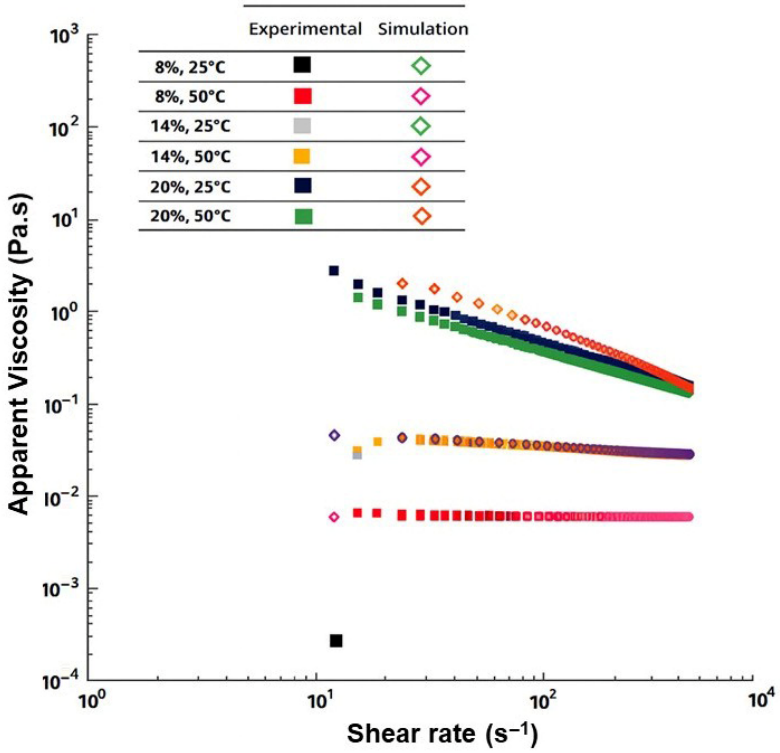


Figure 2. Computed apparent viscosities plotted against shear rate and compared to the experimental apparent viscosities measurements for (8%, 14%, 20%) casein weight per volume percentage fractions and at 25 °C and 50 °C (log scale). The experimental viscosities are plotted in closed/black squares, and open diamonds represent the simulation results with experimental volume fractions. At a shear rate of about 23 s^{-1} and at 25 °C, the relative error between simulation and experiment is approximately 46% at 8% casein (weight/volume fraction) and below 1% at higher concentrations. In the log scale, the discrepancies remain very limited.

A high degree of agreement is observed for the rheological behavior between experiments and simulations, whatever the temperature of the solvent and the casein concentration. The difference in predicted and experimentally determined viscosities is statistically insignificant at a low casein weight per volume (8% *w*/*v*, 14%*w*/*v*) and starts to be visible at 20% *w*/*v*.

Experimentally and in our CG model, no temperature dependence of apparent viscosity up to 14% *w*/*v* has been reported for the covered range of temperature (25 °C and 50 °C). At a casein concentration of 20% *w*/*v*, a slight difference starts to be observed both experimentally and numerically between 25 °C and 50 °C.

Up to 14% casein weight percentage, casein dispersions follow a Newtonian behavior. As expected, when the colloidal casein content increases, shear thinning behavior appears. This has been widely observed in the literature for dispersion models involving hard spheres as colloids in polymer area [67,68] or for casein dispersions [28,41,51,69].

As indicated by Bouchoux et al. [50], the colloidal casein concentrates, even at a low volume fraction, are expected to exhibit non-Newtonian behavior at a high shear rate. Therefore, a shear thinning domain should be observed even as low as 8% *w*/*v*s. It is possible that, under our experimental conditions, the shear rate values are not high enough to induce shear thinning behavior. Nevertheless, Bouchoux et al. [50] observed similar critical casein weight per volume percentages for the onset of shear thinning behavior determined at 400 s^{-1}, namely, around 120 g/L to 138 g/L.

To further estimate the performance of the proposed polydisperse CG model, a set of simulations was carried out to predict the rheological behaviors of the native phosphocaseinate dispersions studied by Bouchoux et al. [50] at the various casein concentrations employed by the authors (10–56–92–121–138–146–158–168 g/L).

In their experimental work, Bouchoux et al. measured the evolution of the apparent viscosity of the casein dispersion (η) versus the shear stress (τ) and showed that a 3-parameter model fits all the apparent viscosity data of the suspension, regardless of the casein volume fraction of the dispersion (precisely, the 3-parameter model is $(\eta-\eta_\infty)/(\eta_0-\eta_\infty) = 1/(1 + \tau/\tau_c)$, where η_∞ is the apparent viscosity at high shear and η_0 is the viscosity at low shear, and τ_c is a characteristic shear stress that defines the shear thinning properties). Consequently, a single master curve (representing normalized apparent viscosity, $(\eta-\eta_\infty)/(\eta_0-\eta_\infty)$, versus normalized shear stress, τ/τ_c), has the ability to gather all the tested dispersions, whatever the casein volume fraction.

Bouchoux et al. also illustrated that the plot of the deduced characteristic shear stress, τ_c, as a function of the casein volume fraction (estimated using a micelle voluminosity of 4.4 mL/g), is a curve that reaches an optimum, located after a linear increase with casein volume fraction and followed by a drastic linear decrease with volume fraction. An identical curve shape was also observed previously by de Kruif et al. [32,70], with an abscissa shift, when studying the rheological behavior of silica dispersions in cyclohexane. The average diameter of the glass sphere was 78 nm with a narrow size distribution and was assumed to mimic the rheology of concentrated suspensions of non-interactive and rigid particles.

Finally, Bouchoux et al. [50] also provided us with a plot of the relative or reduced low-shear apparent viscosity, $\eta_{r,0} = \eta_0/\eta_s$, as a function of the casein volume fraction, ∅ (estimated using micelle voluminosity of 4.4 mL/g) obtained for their dispersions, where η_0 and η_s are, respectively, the viscosity of the dispersion and the viscosity of the solvent at low shear. They showed that $\eta_{r,0}$ could be modeled by Quemada's empirical equation (precisely $\eta_{r,0} = (1-\varnothing/\varnothing_{max,0})^{-2}$) [71], provided that the solid fraction at maximum packing, $\varnothing_{max,0}$, introduced into this equation lies between these two extreme values

known for monodisperse (∅_(max,0) = 0.64) and for 40% polydisperse (∅_(max,0) = 0.71) hard spheres.

On this basis, it was decided to assess the performance of the polydisperse CG model for casein dispersions of Bouchoux et al. [50] by analyzing the similarity existing between experimental and predicted results for the three graphs (Figure 3) initially displayed by these authors representing (i) normalized apparent viscosity, (η-η_∞)/(η_0-η_∞) versus normalized shear stress, τ/τ_c; (ii) shear stress, τ_c, versus casein volume fraction; (iii) relative apparent viscosity at low shear η_(r,0) = η_0/η_s versus casein volume fraction, ∅.

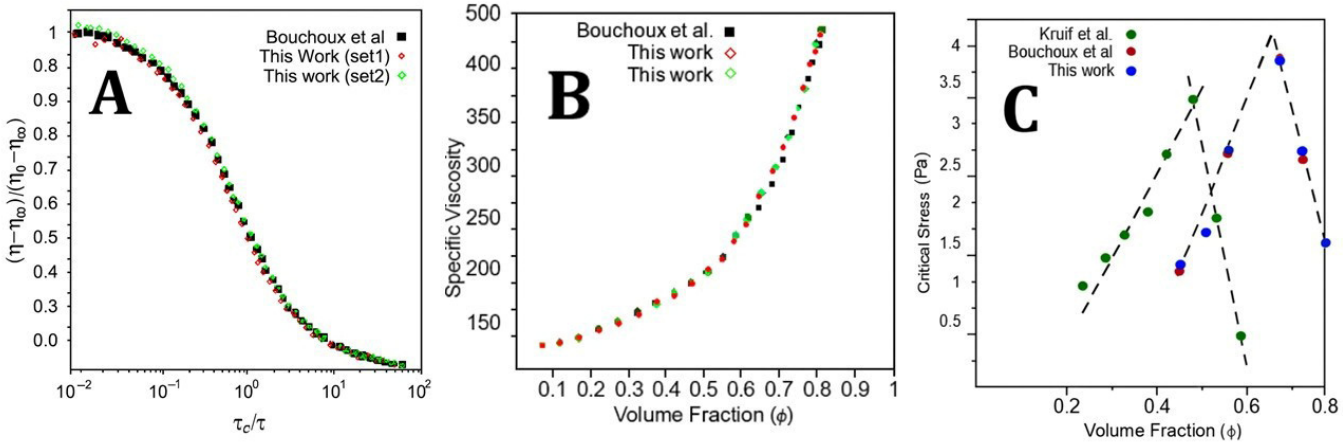


Figure 3. Comparison of predicted and experimental rheological data obtained for PPCN dispersions of Bouchoux et al. [50] and Kruif et al. [32], using the polydisperse CG model: (**A**) reduced viscosity vs. reduced critical stress, (**B**) specific viscosity vs. volume fraction, and (**C**) critical shear stress vs. volume fraction. (**A**–**C**) These results are similar to those presented by Bouchoux et al. in their original publication [50]. At a reduced critical stress of about 0.02, the relative error between simulation and experiment for the normalized apparent viscosity (**A**) is approximately 2.2%.

Once again, an excellent agreement between simulation and experimental rheological data (Figure 3) is highlighted. These results show that the parameters used to define the polydisperse CG model are rather robust. Therefore, the polydisperse CG model seems well suited to capture in vitro the rheological data for a large range of PPCN dispersions; namely, both the shear thinning properties and the strong non-linear increase in apparent viscosity with increasing solid casein fraction (from 10 g/L to 168 g/L) can be predicted.

It is also shown that different compression regimes for the casein can be guessed by the polydisperse CG model (Figure 3B). Again, the model seems robust. Indeed, the predictions are still superimposed with experimental data, even when the size of colloid is changed and dispersions consist of monodisperse beads (as in the case of de Kruif et al.'s data [32]). The fact that the polydisperse CG model predicts a shift for the solid fraction at maximum packing (when switching from data of de Kruif et al. to Bouchoux et al. [32,50]) is rather consistent, since polydispersity is known to lead to higher values for the volume fraction at which the hard-sphere systems are compressed. Although elastic properties are not addressed in this work, it represents a step forward in identifying the liquid/solid transition of casein dispersions.

3.2. Comparison of Predicted and Experimental Data for the Monodisperse CG Model for PPCN Dispersion at 14%

Figure 4 shows the evolution of apparent viscosity vs. shear rate for the native PPCN dispersion at a 14% volume fraction measured by Nogueira [47]. For this dispersion, Nogueira determined the average particle/micelle size to be equal to 206.15 nm. Figure 4 also reports five sets of simulations obtained by the monodisperse CG model with differ-

ent average colloidal particle sizes (196.2, 199.3, 208.3, 212.7, and 214.6 nm), around the measured value of 208 nm. For all fixed average particle/micelle sizes, good agreement is obtained between the experimental and predicted values of the apparent viscosity. Nevertheless, the best agreement in viscosities in the 10–500/s^{-1} range of shear rates were obtained from the simulation with an average particle size of 208.2 nm, suggesting that a precise knowledge of the distribution of casein particle size is not essential and that the key parameter to capture the viscous rheological behavior is the average particle/micelle size. A similar trend was obtained regarding the agreement between experimental and predicted values for the monodisperse CG model at other volume fractions (8% and 14%) reported by Nogueira [47] and Bouchoux et al. [50] when the average particle/micelle size was fixed at 206.15 nm.

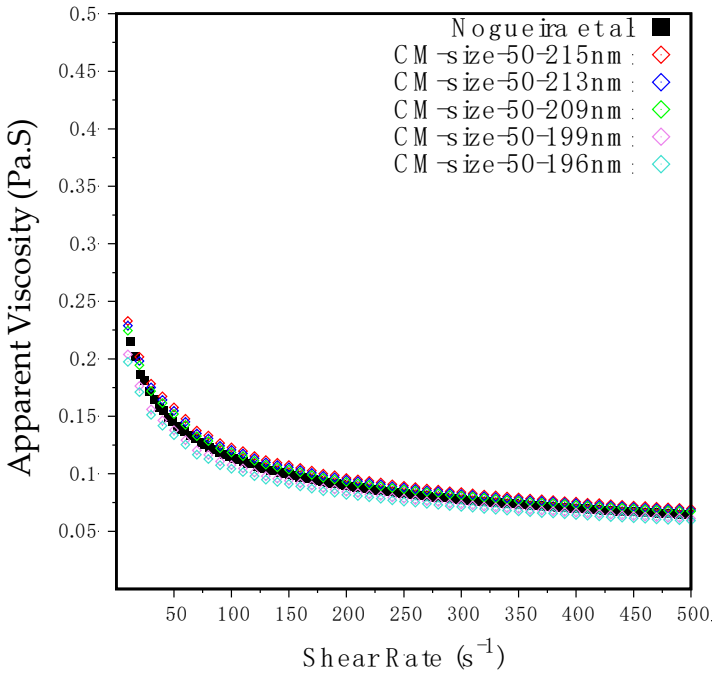


Figure 4. Apparent viscosities plotted against shear rate for the native PPCN dispersion at 14% obtained experimentally [46] and with the monodisperse CG model. The experimental viscosities are plotted in closed/black squares, and open diamonds represent the simulation results with various monomodal particle size. The monomodal particle sizes appearing in the legend have been rounded off to the nearest integer. At a shear rate of about 68 s^{-1} and for the size distribution [50 nm–196 nm], the relative error between simulation and experiment for the normalized apparent viscosity is approximately 7.2%.

3.3. Performance of the Monodisperse CG Model for Demineralized Casein Dispersions

To go further in the validation of the monodisperse CG model, other simulations were carried out for casein dispersions (5%, 10%, and 25% demineralization, for which the average particle/micelle size is known to be different) and were measured (Figure 5).

Nogueira [47,48] reported that upon 5% demineralization, the casein micelles swell and increase in size by 10–20% (average reported size, native = ~208 nm, DM-5% = ~230 nm), while upon higher degrees of demineralization, compression of casein micelles happens at 10% (native = ~208 nm, DM-10% = ~216 nm), and structural deformation and swelling were reported for 25% demineralization (native = ~208 nm, DM-25% = ~204.5).

The simulation results for 5% demineralization are shown in Figure 5A. The average particle sizes considered in the monodisperse CG model size were 216, 221, 222, 230, and 239 nm. The most accommodating results were found to be the viscosities computed

for the particle size 222 nm, which is close to the average particle size measured for the demineralized casein (equal to 230 nm).

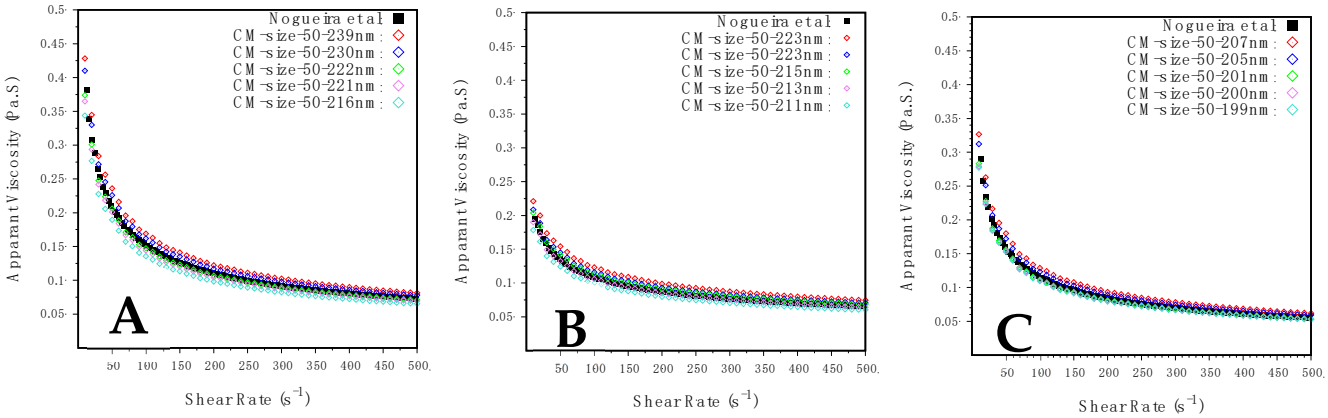


Figure 5. Apparent viscosities plotted against shear rate for demineralized PPCN dispersion at 14%, obtained experimentally and with the monodisperse CG model: (**A**) 5% demineralization, (**B**) 10% demineralization, and (**C**) 25% demineralization. The experimental viscosities are plotted in closed/black squares, and open diamonds represent the simulation results with various monomodal particle sizes. The monomodal particle sizes appearing in the legend have been rounded off to the nearest integer. At a shear rate of about 139 s^{-1} and for 5% demineralization (**A**), the relative error between simulation and experiment for the normalized apparent viscosity is approximately 16.7%.

Similarly, the prediction of apparent viscosity for 10% and 25% demineralized casein dispersions obtained with the monodisperse CG model is satisfactory when the average size of casein particle is close to those measured (DM-10% = ~216 nm and DM-25% = ~204.5 nm).

Regarding the simulations for a polydisperse colloidal system with an average particle window of 50–239 nm and with varying averages for native, 5%, 10%, and 25% demineralization, the agreement between experimentally measured and computed viscosities is better than the monodisperse simulation system. This improvement of computed viscosities can be attributed to the pseudo-polydispersity, which changes the particle packing in the colloidal suspension. Lower and upper bounds of the liquid–solid transition volume fraction of 0.64 and 0.78 were reported by Bouchoux et al. [50], considering mono- and polydispersity of the colloidal suspension of casein micelles.

4. Conclusions

In this work, we have carried out molecular dynamics studies, particularly non-equilibrium molecular dynamics (NEMD) simulations, to study the rheological behavior of rehydrated casein colloidal suspensions at various volume fractions of interest to the food industry for the production of HP beverages.

We have built Coarse-Grained (CG) models that only include colloid–colloid interactions to study the rheological behavior of colloidal suspensions, namely, their viscous properties. Inter-particle interactions play an important role in the rheological behavior of colloidal suspensions. In this work, the interactions between different types of particles were represented using the basic, purely repulsive WCA potential. As shown in previous literature studies, the local structure of the colloidal systems (e.g., aggregation/dispersion) can be tuned by changing the length scale of different interactions in the system.

The two proposed CG models (polydisperse and monodisperse) successfully predict the rheology of casein dispersions, proving that CG models with explicit solvent molecules are adequate. A better prediction is obtained when the colloid distribution is implemented in the CG model. Nevertheless, when this distribution is not known a priori, an average

dimension of the casein particle is enough, proving that this physical quantity is the key input parameter to consider. These preliminary CG models pave the way. For example, the model used in this work can be readily extended by incorporating appropriate intermolecular interactions (e.g., electrostatic interactions) between particles in the case where the interactions in the system are strong and one wishes to study the effects of a specific chemistry on the structure, as well as the rheology of a particular nanocolloidal suspension. Such a study can be carried out using detailed atomistic models of nanocolloidal systems and incorporating hydrodynamic interactions and long-range forces. However, this ability to handle specific interactions and short-range structure comes with a potentially severe increase in the computational cost of the simulations compared to the cost of mesoscopic simulation techniques such as BD and SD, which use a continuum representation of the solvent. The use of an explicit solvent model will be useful when specific chemical interactions and nanoscale molecular structure play an important role in the rheology of the system, making a continuum treatment of the solvent inadequate. For complex fluid systems where both nanoscale and mesoscale effects are important, the results of these model simulations could be used as an input for mesoscale simulation techniques such as BD or SD simulations.

Author Contributions: Conceptualization, G.D., R.P.S., F.A., P.P. and S.B.; Methodology, R.P.S., G.D. and F.A.; Validation, G.D., P.P., S.B., R.P.S. and F.A.; Writing—Original Draft Preparation, R.P.S.; Writing—Review and Editing, G.D., F.A., P.P. and S.B.; Supervision, G.D., S.B. and F.A.; Project Administration, G.D. and M.H.; Funding Acquisition, G.D. All authors have read and agreed to the published version of the manuscript.

Funding: This study has been led within the frame of the project "Proteinolab", a partnership between the Institut National de Recherche pour l'Agriculture, l'Alimentation et l'Environnement (INRAE) and Ingredia Dairy Experts. The "Proteinolab" project was supported by the French National Research Agency (ANR) (Project ANR-17-LCV2-0005-01 Labcom), allowing Postdoctoral training of RPS at INRAE/UMET, Lille. This project was also co-funded by the European Union with the European Regional Development Fund (FEDER-FSE 2014–2020: NP0023283) to enable us to consolidate the preliminary results obtained for molecular dynamic simulation and academic–industrial partnership. The authors also would like to thank the ANR-financed "ProteinoPepS" project, which enabled us to strengthen scientific discussion about the valorization of this work. RPS acknowledge the CEA-CURIE HPC for computing resources. All the simulations were performed using CEA-CURIE resources on IRENE and CINES computing clusters.

Institutional Review Board Statement: Not applicable.

Informed Consent Statement: Not applicable.

Data Availability Statement: The data are available upon request to the authors.

Conflicts of Interest: Author Manon Hiolle was employed by the company Ingredia. The remaining authors declare that the research was conducted in the absence of any commercial or financial relationships that could be construed as a potential conflict of interest.

Abbreviations

The following abbreviations are used in this manuscript:

BD	Brownian dynamics
CCPs	colloidal calcium phosphate clusters
CG	Coarse-Grained
CM	Casein micelle
DPD	Dissipative particle dynamics
FLD	Fast lubrication dynamics

HP	Hyper-Protein
LB	Lattice Boltzmann
LJ	Lennard-Jones
MD	molecular dynamics
SD	Stokesian dynamics
SRD	Stochastic rotation dynamics
WCA	Weeks–Chandler–Andersen

References

1. Lagrange, V.; Whitsett, D.; Burris, C. Global Market for Dairy Proteins. *J. Food Sci.* **2015**, *80*, A16–A22. [CrossRef]
2. Bouvier, J.-M.; Collado, M.; Gardiner, D.; Scott, M.; Schuck, P. Physical and Rehydration Properties of Milk Protein Concentrates: Comparison of Spray-Dried and Extrusion-Porosified Powders. *Dairy Sci. Technol.* **2013**, *93*, 387–399. [CrossRef]
3. Bijl, E.; Van Valenberg, H.J.F.; Huppertz, T.; Van Hooijdonk, A.C.M. Protein, Casein, and Micellar Salts in Milk: Current Content and Historical Perspectives. *J. Dairy Sci.* **2013**, *96*, 5455–5464. [CrossRef] [PubMed]
4. Bingham, E.W.; Farrell, H.M. Phosphorylation of Casein by the Lactating Mammary Gland: A Review. *J. Dairy Sci.* **1977**, *60*, 1199–1207. [CrossRef]
5. Fox, P.F.; Brodkorb, A. The Casein Micelle: Historical Aspects, Current Concepts and Significance. *Int. Dairy J.* **2008**, *18*, 677–684. [CrossRef]
6. Gaucheron, F. The Minerals of Milk. *Reprod. Nutr. Dev.* **2005**, *45*, 473–483. [CrossRef] [PubMed]
7. Holt, C. Structure and Stability of Bovine Casein Micelles. In *Advances in Protein Chemistry*; Elsevier: Amsterdam, The Netherlands, 1992; Volume 43, pp. 63–151, ISBN 978-0-12-034243-3.
8. Lucey, J.A.; Otter, D.; Horne, D.S. A 100-Year Review: Progress on the Chemistry of Milk and Its Components. *J. Dairy Sci.* **2017**, *100*, 9916–9932. [CrossRef] [PubMed]
9. Verruck, S.; Balthazar, C.F.; Rocha, R.S.; Silva, R.; Esmerino, E.A.; Pimentel, T.C.; Freitas, M.Q.; Silva, M.C.; Da Cruz, A.G.; Prudencio, E.S. Dairy Foods and Positive Impact on the Consumer's Health. In *Advances in Food and Nutrition Research*; Elsevier: Amsterdam, The Netherlands, 2019; Volume 89, pp. 95–164, ISBN 978-0-12-817171-4.
10. Chandan, R.C.; O'Rell, K. Ingredients for Yogurt Manufacture. In *Manufacturing Yogurt and Fermented Milks*; Chandan, R.C., Kilara, A., Eds.; Wiley: Hoboken, NJ, USA, 2013; pp. 217–237, ISBN 978-1-119-96708-8.
11. Sodini, I.; Tong, P. Milk and Milk-Based Dairy Ingredients. In *Manufacturing Yogurt and Fermented Milks*; Chandan, R.C., Kilara, A., Eds.; Wiley: Hoboken, NJ, USA, 2013; pp. 167–178, ISBN 978-1-119-96708-8.
12. Wilborn, C.D.; Taylor, L.W.; Outlaw, J.; Williams, L.; Campbell, B.; Foster, C.A.; Smith-Ryan, A.; Urbina, S.; Hayward, S. The Effects of Pre- and Post-Exercise Whey vs. Casein Protein Consumption on Body Composition and Performance Measures in Collegiate Female Athletes. *J. Sports Sci. Med.* **2013**, *12*, 74–79. [CrossRef]
13. Freudig, B.; Hogekamp, S.; Schubert, H. Dispersion of Powders in Liquids in a Stirred Vessel. *Chem. Eng. Process. Process Intensif.* **1999**, *38*, 525–532. [CrossRef]
14. Nasser, S.; Jeantet, R.; De-Sa-Peixoto, P.; Ronse, G.; Nuns, N.; Pourpoint, F.; Burgain, J.; Gaiani, C.; Hédoux, A.; Delaplace, G. Microstructure Evolution of Micellar Casein Powder upon Ageing: Consequences on Rehydration Dynamics. *J. Food Eng.* **2017**, *206*, 57–66. [CrossRef]
15. Richard, B.; Le Page, J.F.; Schuck, P.; Andre, C.; Jeantet, R.; Delaplace, G. Towards a Better Control of Dairy Powder Rehydration Processes. *Int. Dairy J.* **2013**, *31*, 18–28. [CrossRef]
16. McSweeney, D.J.; O'Mahony, J.A.; McCarthy, N.A. Strategies to Enhance the Rehydration Performance of Micellar Casein-Dominant Dairy Powders. *Int. Dairy J.* **2021**, *122*, 105116. [CrossRef]
17. Bergman, P.; Brighenti, S. Targeted Nutrition in Chronic Disease. *Nutrients* **2020**, *12*, 1682. [CrossRef]
18. Abdallah, M.; Azevedo-Scudeller, L.; Hiolle, M.; Lesur, C.; Baniel, A.; Delaplace, G. Review on Mechanisms Leading to Fouling and Stability Issues Related to Heat Treatment of Casein-Based RTD Beverages. *Food Bioprod. Process.* **2022**, *136*, 67–83. [CrossRef]
19. Abdallah, M.; Azevedo-Scudeller, L.; Sun, W.; Descamps, A.; Gourdin, P.; Hiolle, M.; Baniel, A.; Lesur, C.; Delaplace, G. Impact of Casein Demineralization on the Fouling of UHT Plant and the Heat Stability of High Protein Beverages: A Pilot Scale Study. *Food Bioprod. Process.* **2023**, *137*, 45–55. [CrossRef]
20. Corredig, M.; Nair, P.K.; Li, Y.; Eshpari, H.; Zhao, Z. Invited Review: Understanding the Behavior of Caseins in Milk Concentrates. *J. Dairy Sci.* **2019**, *102*, 4772–4782. [CrossRef]
21. Pandalaneni, K.; Amamcharla, J.K.; Marella, C.; Metzger, L.E. Influence of Milk Protein Concentrates with Modified Calcium Content on Enteral Dairy Beverage Formulations: Physicochemical Properties. *J. Dairy Sci.* **2018**, *101*, 9714–9724. [CrossRef]
22. Orrù, S.; Imperlini, E.; Nigro, E.; Alfieri, A.; Cevenini, A.; Polito, R.; Daniele, A.; Buono, P.; Mancini, A. Role of Functional Beverages on Sport Performance and Recovery. *Nutrients* **2018**, *10*, 1470. [CrossRef]

23. Arenas-Jal, M.; Suñé-Negre, J.M.; Pérez-Lozano, P.; García-Montoya, E. Trends in the Food and Sports Nutrition Industry: A Review. *Crit. Rev. Food Sci. Nutr.* **2020**, *60*, 2405–2421. [CrossRef]
24. Cintineo, H.P.; Arent, M.A.; Antonio, J.; Arent, S.M. Effects of Protein Supplementation on Performance and Recovery in Resistance and Endurance Training. *Front. Nutr.* **2018**, *5*, 83. [CrossRef] [PubMed]
25. Lochlainn, M.N.; Bowyer, R.C.E.; Steves, C.J. Dietary Protein and Muscle in Aging People: The Potential Role of the Gut Microbiome. *Nutrients* **2018**, *10*, 929. [CrossRef]
26. Raak, N.; Pedersen, J.S.; Corredig, M. Structural and Colloidal Changes of Casein Micelles Induced by Membrane Concentration and Their Dependence on the Milieu Exchange Conditions. *Colloids Surf. A Physicochem. Eng. Asp.* **2023**, *670*, 131580. [CrossRef]
27. Møller, T.L.; Nielsen, S.B.; Pedersen, J.S.; Corredig, M. Structural and Compositional Characterization of Ca- and β-Casein Enriched Casein Micelles. *Food Hydrocoll.* **2024**, *151*, 109811. [CrossRef]
28. Bienvenue, A.; Jiménez-Flores, R.; Singh, H. Rheological Properties of Concentrated Skim Milk: Importance of Soluble Minerals in the Changes in Viscosity During Storage. *J. Dairy Sci.* **2003**, *86*, 3813–3821. [CrossRef]
29. Meletharayil, G.H.; Patel, H.A.; Metzger, L.E.; Marella, C.; Huppertz, T. Influence of Partially Demineralized Milk Proteins on Rheological Properties and Microstructure of Acid Gels. *J. Dairy Sci.* **2018**, *101*, 1864–1871. [CrossRef]
30. Nogueira, M.; Humblot, L.; Singh, R.P.; Dieude-Fauvel, E.; Doumert, B.; Nasser, S.; Lesur, C.; Karoui, R.; Delaplace, G.; Peixoto, P.P.S. The Heterogeneous Substructure of Casein Micelles Evidenced by SAXS and NMR in Demineralized Samples. *Food Hydrocoll.* **2021**, *117*, 106653. [CrossRef]
31. Wusigale; Liang, L.; Luo, Y. Casein and Pectin: Structures, Interactions, and Applications. *Trends Food Sci. Technol.* **2020**, *97*, 391–403. [CrossRef]
32. De Kruif, C.G.; Huppertz, T.; Urban, V.S.; Petukhov, A.V. Casein Micelles and Their Internal Structure. *Adv. Colloid Interface Sci.* **2012**, *171–172*, 36–52. [CrossRef]
33. Rose, D.; Colvin, J.R. Internal Structure of Casein Micelles from Bovine Milk. *J. Dairy Sci.* **1966**, *49*, 351–355. [CrossRef]
34. Smith, G.N.; Brok, E.; Christiansen, M.V.; Ahrné, L. Casein Micelles in Milk as Sticky Spheres. *Soft Matter* **2020**, *16*, 9955–9963. [CrossRef]
35. Horne, D.S. Casein Micelle Structure: Models and Muddles. *Curr. Opin. Colloid Interface Sci.* **2006**, *11*, 148–153. [CrossRef]
36. Beliciu, C.M.; Moraru, C.I. Effect of Solvent and Temperature on the Size Distribution of Casein Micelles Measured by Dynamic Light Scattering. *J. Dairy Sci.* **2009**, *92*, 1829–1839. [CrossRef]
37. Bijl, E.; De Vries, R.; Van Valenberg, H.; Huppertz, T.; Van Hooijdonk, T. Factors Influencing Casein Micelle Size in Milk of Individual Cows: Genetic Variants and Glycosylation of κ-Casein. *Int. Dairy J.* **2014**, *34*, 135–141. [CrossRef]
38. Hemar, Y.; Xu, C.; Wu, S.; Ashokkumar, M. Size Reduction of "Reformed Casein Micelles" by High-Power Ultrasound and High Hydrostatic Pressure. *Ultrason. Sonochem.* **2020**, *63*, 104929. [CrossRef] [PubMed]
39. Dalgleish, D.G. On the Structural Models of Bovine Casein Micelles—Review and Possible Improvements. *Soft Matter* **2011**, *7*, 2265–2272. [CrossRef]
40. Rebouillat, S.; Ortega-Requena, S. Potential Applications of Milk Fractions and Valorization of Dairy By-Products: A Review of the State-of-the-Art Available Data, Outlining the Innovation Potential from a Bigger Data Standpoint. *J. Biomater. Nanobiotechnol.* **2015**, *6*, 176–203. [CrossRef]
41. Bouchoux, A.; Ventureira, J.; Gésan-Guiziou, G.; Garnier-Lambrouin, F.; Qu, P.; Pasquier, C.; Pézennec, S.; Schweins, R.; Cabane, B. Structural Heterogeneity of Milk Casein Micelles: A SANS Contrast Variation Study. *Soft Matter* **2015**, *11*, 389–399. [CrossRef] [PubMed]
42. McMahon, D.J.; Oommen, B.S. Supramolecular Structure of the Casein Micelle. *J. Dairy Sci.* **2008**, *91*, 1709–1721. [CrossRef]
43. Huppertz, T.; Gazi, I.; Luyten, H.; Nieuwenhuijse, H.; Alting, A.; Schokker, E. Hydration of Casein Micelles and Caseinates: Implications for Casein Micelle Structure. *Int. Dairy J.* **2017**, *74*, 1–11. [CrossRef]
44. Phadungath, C. Casein Micelle Structure: A Concise Review. *Songklanakarin J. Sci. Technol.* **2005**, *27*, 201–212.
45. Broyard, C.; Gaucheron, F. Modifications of Structures and Functions of Caseins: A Scientific and Technological Challenge. *Dairy Sci. Technol.* **2015**, *95*, 831–862. [CrossRef]
46. Nogueira, M.H.; Ben-Harb, S.; Schmutz, M.; Doumert, B.; Nasser, S.; Derensy, A.; Karoui, R.; Delaplace, G.; Peixoto, P.P.S. Multiscale Quantitative Characterization of Demineralized Casein Micelles: How the Partial Excision of Nano-Clusters Leads to the Aggregation during Rehydration. *Food Hydrocoll.* **2020**, *105*, 105778. [CrossRef]
47. Nogueira, M. Relation Between Structure and Viscosity in Demineralized Casein Micelles. Ph.D. Thesis, University of Lille, Lille, France, 2020.
48. Nogueira, M.H.; Scudeler, L.A.; Humblot, L.; Doumert, B.; Hennetier, M.; Violleau, F.; Lesur, C.; Delaplace, G.; Peixoto, P.P.S. Assessment of Structures in Phosphocaseinate Dispersions by A4F, NMR and SAXS: The Impact of Demineralization and Heat Treatment on Viscosity. *Food Hydrocoll.* **2023**, *137*, 108366. [CrossRef]
49. Pedersen, J.S.; Møller, T.L.; Raak, N.; Corredig, M. A Model on an Absolute Scale for the Small-Angle X-Ray Scattering from Bovine Casein Micelles. *Soft Matter* **2022**, *18*, 8613–8625. [CrossRef]

50. Bouchoux, A.; Debbou, B.; Gésan-Guiziou, G.; Famelart, M.-H.; Doublier, J.-L.; Cabane, B. Rheology and Phase Behavior of Dense Casein Micelle Dispersions. *J. Chem. Phys.* **2009**, *131*, 165106. [CrossRef]
51. Dahbi, L.; Alexander, M.; Trappe, V.; Dhont, J.K.G.; Schurtenberger, P. Rheology and Structural Arrest of Casein Suspensions. *J. Colloid Interface Sci.* **2010**, *342*, 564–570. [CrossRef]
52. Dickinson, E. Structure and Rheology of Colloidal Particle Gels: Insight from Computer Simulation. *Adv. Colloid Interface Sci.* **2013**, *199–200*, 114–127. [CrossRef] [PubMed]
53. Groot, R.D.; Warren, P.B. Dissipative Particle Dynamics: Bridging the Gap between Atomistic and Mesoscopic Simulation. *J. Chem. Phys.* **1997**, *107*, 4423–4435. [CrossRef]
54. Pryamitsyn, V.; Ganesan, V. A Coarse-Grained Explicit Solvent Simulation of Rheology of Colloidal Suspensions. *J. Chem. Phys.* **2005**, *122*, 104906. [CrossRef] [PubMed]
55. Padding, J.T.; Louis, A.A. Hydrodynamic Interactions and Brownian Forces in Colloidal Suspensions: Coarse-Graining over Time and Length Scales. *Phys. Rev. E* **2006**, *74*, 031402. [CrossRef]
56. Carpen, I.C.; Brady, J.F. Microrheology of Colloidal Dispersions by Brownian Dynamics Simulations. *J. Rheol.* **2005**, *49*, 1483–1502. [CrossRef]
57. Ermak, D.L.; McCammon, J.A. Brownian Dynamics with Hydrodynamic Interactions. *J. Chem. Phys.* **1978**, *69*, 1352–1360. [CrossRef]
58. Brady, J.F.; Bossis, G. Stokesian Dynamics. *Annu. Rev. Fluid Mech.* **1988**, *20*, 111–157. [CrossRef]
59. Malevanets, A.; Kapral, R. Solute Molecular Dynamics in a Mesoscale Solvent. *J. Chem. Phys.* **2000**, *112*, 7260–7269. [CrossRef]
60. Kumar, A.; Higdon, J.J.L. Origins of the Anomalous Stress Behavior in Charged Colloidal Suspensions under Shear. *Phys. Rev. E* **2010**, *82*, 051401. [CrossRef]
61. Devarajan, D.; Nourian, P.; McKenna, G.B.; Khare, R. Molecular Simulation of Nanocolloid Rheology: Viscosity, Viscoelasticity, and Time-Concentration Superposition. *J. Rheol.* **2020**, *64*, 529–543. [CrossRef]
62. in'T Veld, P.J.; Plimpton, S.J.; Grest, G.S. Accurate and Efficient Methods for Modeling Colloidal Mixtures in an Explicit Solvent Using Molecular Dynamics. *Comput. Phys. Commun.* **2008**, *179*, 320–329. [CrossRef]
63. Plimpton, S. Fast Parallel Algorithms for Short-Range Molecular Dynamics. *J. Comput. Phys.* **1995**, *117*, 1–19. [CrossRef]
64. Todd, B.D.; Daivis, P.J. *Nonequilibrium Molecular Dynamics: Theory, Algorithms and Applications*, 1st ed.; Cambridge University Press: Cambridge, UK, 2017; ISBN 978-0-521-19009-1.
65. Evans, D.J.; Morriss, G. *Statistical Mechanics of Nonequilibrium Liquids*, 2nd ed.; Cambridge University Press: Cambridge, UK, 2008; ISBN 978-0-521-85791-8.
66. Khabaz, F.; Khare, R. Molecular Simulations of Asphalt Rheology: Application of Time–Temperature Superposition Principle. *J. Rheol.* **2018**, *62*, 941–954. [CrossRef]
67. Poslinski, A.J.; Ryan, M.E.; Gupta, R.K.; Seshadri, S.G.; Frechette, F.J. Rheological Behavior of Filled Polymeric Systems I. Yield Stress and Shear-Thinning Effects. *J. Rheol.* **1988**, *32*, 703–735. [CrossRef]
68. Poslinski, A.J.; Ryan, M.E.; Gupta, R.K.; Seshadri, S.G.; Frechette, F.J. Rheological Behavior of Filled Polymeric Systems II. The Effect of a Bimodal Size Distribution of Particulates. *J. Rheol.* **1988**, *32*, 751–771. [CrossRef]
69. Doudiès, F.; Arsène, A.-S.; Garnier-Lambrouin, F.; Famelart, M.-H.; Bouchoux, A.; Pignon, F.; Gésan-Guiziou, G. Major Role of Voluminosity in the Compressibility and Sol-Gel Transition of Casein Micelle Dispersions Concentrated at 7 °C and 20 °C. *Foods* **2019**, *8*, 652. [CrossRef]
70. De Kruif, C.G.; Van Iersel, E.M.F.; Vrij, A.; Russel, W.B. Hard Sphere Colloidal Dispersions: Viscosity as a Function of Shear Rate and Volume Fraction. *J. Chem. Phys.* **1985**, *83*, 4717–4725. [CrossRef]
71. Quemada, D. Rheology of Concentrated Disperse Systems II. A Model for Non-Newtonian Shear Viscosity in Steady Flows. *Rheol. Acta* **1978**, *17*, 632–642. [CrossRef]

Disclaimer/Publisher's Note: The statements, opinions and data contained in all publications are solely those of the individual author(s) and contributor(s) and not of MDPI and/or the editor(s). MDPI and/or the editor(s) disclaim responsibility for any injury to people or property resulting from any ideas, methods, instructions or products referred to in the content.